

Structural reliability of reinforced concrete buildings under earthquakes and corrosion effects

Juan Bojórquez^a, Sandra Ponce^a, Sonia E. Ruiz^b, Edén Bojórquez^{a,*}, Alfredo Reyes-Salazar^a, Manuel Barraza^c, Robespierre Chávez^a, Federico Valenzuela^a, Herian Leyva^a, Victor Baca^a

^a Facultad de Ingeniería, Universidad Autónoma de Sinaloa, Calzada de las Américas y B. Universitarios s/n, C.P. 80040 Culiacán, Sinaloa, Mexico

^b Universidad Nacional Autónoma de México, Ciudad Universitaria, Del. Coyoacán, C.P. 04510 Mexico City, Mexico

^c Facultad de Ingeniería, Arquitectura y Diseño, Universidad Autónoma de Baja California, C.P. 22860 Ensenada, Mexico

ARTICLE INFO

Keywords:

Structural reliability
Corrosion
Stochastic modelling
Reinforced concrete building
Earthquake ground motions

ABSTRACT

The corrosion process due to the erosion of chloride ions on reinforced concrete (RC) buildings is analyzed in this paper. The main objective of this study is to determine the influence of the corrosion on structural reliability of reinforced concrete buildings under earthquakes. It is assumed that the buildings are located in the city of Acapulco Guerrero in Mexico, and a comparison of the structural reliability when the resistance of the structural members of the buildings under earthquakes is affected by corrosion and when not is computed. In addition, the influence of concrete cover is considered. For the objective of this study, the buildings are modeled as 3D RC frames and they are subjected to several earthquake ground motion records. Furthermore, the analyses are performed by the Monte Carlo simulation technique and stochastic modelling of corrosion initiation, corrosion propagation and corrosion cracking to estimate the steel corrosion. It is shown that omitting the effect of corrosion in reinforced concrete structures can lead to erroneous estimations of the structural reliability of buildings under earthquakes.

1. Introduction

Nowadays reinforced concrete structures are one of the most common structural systems used around the world. The mix of the high compression strength and the excellent mechanical properties added by the steel made it the ideal compound material to be used in structural applications [1]. However, structures made with that material and exposed for some time to aggressive agents like in coastal areas and places with high contamination levels or places with extreme environmental changes with cycles of freezing/thawing are more susceptible to failure by corrosion [2]. The oxidation of metallic reinforcement due to the erosion of chloride ions can affect significantly the concrete's functional characteristics, like its adherence, also it induces the fissure creations and the concrete's pieces detachments, which influences on the structural performance [3]. In addition, corrosion reduces the reinforced transversal section, achieving an influence in the structural reliability [4]. The corrosion effect in the seismic performance of structures has been studied in the past [5]. Bossio et al. [6] pointed out that corrosion in the stirrups may lead to brittle failures in the most

stressed elements of a structure. In addition, they proposed a retrofit scheme using High Performance Concretes in order to recover the bending capacity and ductility of the structural members. Rizzo et al. [7] developed a time-dependent model to predict the corrosion wastage thickness on historical metal structures. It was observed that, as the corrosion ratio increases, the lateral load and the deformation capacity of the frames, as well as energy dissipation, decrease significantly. Furthermore, the inclusion of innovative structural systems to improve the seismic performance of buildings is becoming a common practice. Among these systems are the buckling-restrained braces (BRB) [8], shear panels [9,10] and friction dampers [11]. These metallic devices could be affected by corrosion when implemented in buildings close to coastal areas. The properties deterioration due to this phenomenon along the structures useful life is a serious problem with high economic implications; for this reason, it must be guaranteed that this type of structures has suitable reliability levels for the collapse and serviceability limit states. In this study an action to reduce social and economic problems due to this phenomenon is to provide tools to measure the variation in the structural reliability levels taking into consideration that

* Corresponding author.

E-mail address: eden@uas.edu.mx (E. Bojórquez).

<https://doi.org/10.1016/j.engstruct.2021.112161>

Received 30 September 2020; Received in revised form 6 January 2021; Accepted 27 February 2021

Available online 26 March 2021

0141-0296/© 2021 Elsevier Ltd. All rights reserved.



Fig. 1. Main characteristics of the corrosion effects in Mexico [31].

the structural capacity and the structural demand vary in a time interval due to corrosion in a high seismic hazard zone. The main structural design goal is to minimize the infrastructure total costs without compromise the behavior requirements and the self-functionality. The structural deterioration becomes a problem when the long time of the structures is considered. Thus, in the analysis and design process it is important to consider the structure useful life. The steel reinforcement corrosion significantly affects the structural performance, affecting the adherence with concrete, causing cracking in the section or even reaching the detachments of concrete pieces [12–14]. Therefore, in this research a study of two reinforced concrete buildings located in Acapulco, Guerrero is conducted. A comparison of the structural reliability of the buildings when the degradation by corrosion is considered and when is not considered in exterior beams and columns is performed. It is shown that omitting the corrosion effects in structures can bring us to a wrong estimation of structural reliability levels in buildings. The structural reliability of chloride-induced corrosion has been studied in many papers. A time-dependent reliability analysis of existing reinforced concrete beams was studied by Firouzi et al. [15]. Shin et al. [16] developed a probability-based durability design software for concrete structures subjected to chloride exposed environments. Ryan and O'Connor [17] studied a probabilistic analysis of the time to chloride-induced corrosion for different self-compacting concretes. Nogueira and Leonel [18] applied probabilistic models to estimate the safety of reinforced concrete structures subjected to chloride ingress. Akiyama et al. [19] estimated the life-cycle reliability of RC bridges piers under seismic and airborne chloride hazards. However, the penetration of harmful ions was only considered with a simple diffusion equation and the boundary concentration of chloride was considered as deterministic or a normal random variable so that the combined effect of harsh environmental aggressiveness and extreme loading conditions is still not very well-understood as a time variant formulation [20–22]. This means that none of the above-mentioned probabilistic models can be used for RC deterioration assessment under a deicing salt environment. In this paper, a stochastic modelling of corrosion initiation, corrosion propagation and corrosion cracking to estimate the steel corrosion is used to compute the structural reliability of complex 3D reinforced concrete buildings located in a high seismic hazard zone of Mexico. For the sake of simplicity and computational effort only the harmful ion penetration is considered with a diffusion equation and the chloride binding capacity, convection, temperature and humidity are not considered.

2. The corrosion process

Concrete is a highly alkaline material (pH between 12.6 and 13.8), due to calcium, sodium and potassium hydroxides. Under this pH condition, the reinforcement steel creates a passive layer that, despite being a few nanometers of thickness, it presents a protection action [23]. However, aggressive agents such as ions chlorides and CO₂, which produces a depassivation on the reinforcing steel bars, could destroy this layer. The initiation of corrosion is generally due to the penetration of free chloride ions, carbonation, or their combined effect [24]. Some studies have shown that the effect of temperature and humidity is significant [25]. Other works conclude that the structural capacity of RC elements would decrease rapidly after the steel reinforcements get depassivated [26]. The load capacity of the RC is seriously reduced after the extender corrosion exceeds a certain limit; for this reason, in this study a probabilistic analysis of corroded RC buildings is very useful for service life and structural failure predictions.

2.1. Chlorides penetration

The corrosion induced by chlorides is mainly present in structures exposed to a marine environment. The chlorides ions are present in marine water; however, wind move them in the breezeway and deposit them in structures that are near to the sea. The chloride ion penetration in concrete is difficult to model, but it seems to be a general agreement that Fick's Law diffusion is superior to other techniques [27]. If the chlorides concentration CO^2 present in the concrete surface and the diffusion coefficient D_C for concrete is supposed independent in space and time, it could be represented with this law as a function of the concrete cover thickness and time, as indicated in Eq. (1):

$$\frac{\partial C(x,t)}{\partial t} = D_C \frac{\partial^2 C(x,t)}{\partial x^2} \quad (1)$$

where (x, t) is the chlorides ion concentration, given as a percentage by weight of cement, at a distance of x meters from the concrete surface after t seconds exposed to a chloride source; and D_C is the chloride diffusion coefficient expressed in m²/sec. The solution to the differential equation is given by:

$$C(x,t) = C_0 \left[1 - \operatorname{erf} \left(\frac{x}{2\sqrt{D_C t}} \right) \right] \quad (2)$$

Table 1
Parameter characteristics of the random variables in corrosion.

Deterioration level: Low	Diffusion coefficient	D_c	N (25.0,2.5) [mm ² /year]
	Surface chloride concentration	C_0	N (0.575,0.038) [%]
	Corrosion density	i_{corr}	Uniform [1.0,2.0] [mA/cm ²]
Deterioration level: Medium	Diffusion coefficient	D_c	N (30.0,2.5) [mm ² /year]
	Surface chloride concentration	C_0	N (0.65,0.038) [%]
	Corrosion density	i_{corr}	Uniform [1.5,2.5] [mA/cm ²]
Deterioration level: High	Diffusion coefficient	D_c	N (35.0,2.5) [mm ² /year]
	Surface chloride concentration	C_0	N (0.725,0.038) [%]
	Corrosion density	i_{corr}	Uniform [2.0,3.0] [mA/cm ²]

where C_0 is the balanced chloride's concentration in the concrete surface, expressed by concrete weight percentage; and erf is the error function.

2.2. Corrosion initiation time

The corrosion initiation time can be estimated in a concrete building considering a chloride corrosion threshold C_{cr} , and d as the cover

thickness; then, the time where the corrosion begins T_i , can be calculated using Eq. (3) [28]:

$$T_i = \frac{d^2}{4D_c} \left[erf^{-1} \left(\frac{C_{cr} - C_0}{C_i - C_0} \right) \right]^2 \quad (3)$$

Based on Eq. (3), outcomes of the corrosion initiation time T_i have been performed using the Monte Carlo simulation; the values of different parameters for the initial surface chloride concentration, the diffusion coefficient for concrete and the corrosion density have been proposed by Thoft-Christensen [29] for three deterioration levels: low, medium, and high. Corrosion is inherently affected by many factors as stated earlier, so it is best modeled as a Gaussian process [30]. The first-passage probability is calculated by estimating the out-crossing rate because corrosion is considered as a Normal stochastic process. The studies conducted by Cook et al. [31] show the corrosion levels in Mexico; the study summary is illustrated in Fig. 1, this map takes into account only chloride related to corrosion based on proximity to the ocean. As shown in the map, the city of Acapulco has a moderate corrosion with high chloride levels so these values are considered for the analysis. The range of values for each deterioration level is represented via normal and uniform probability distributions, which are shown in Table 1.

The strength is primarily attributed to a loss of steel cross section over time [32]. For a reinforced concrete section with reinforcing bars of equal diameter and assuming the same corrosion initiation time for each bar, the area reduction over time can be estimated using Eq. (4).

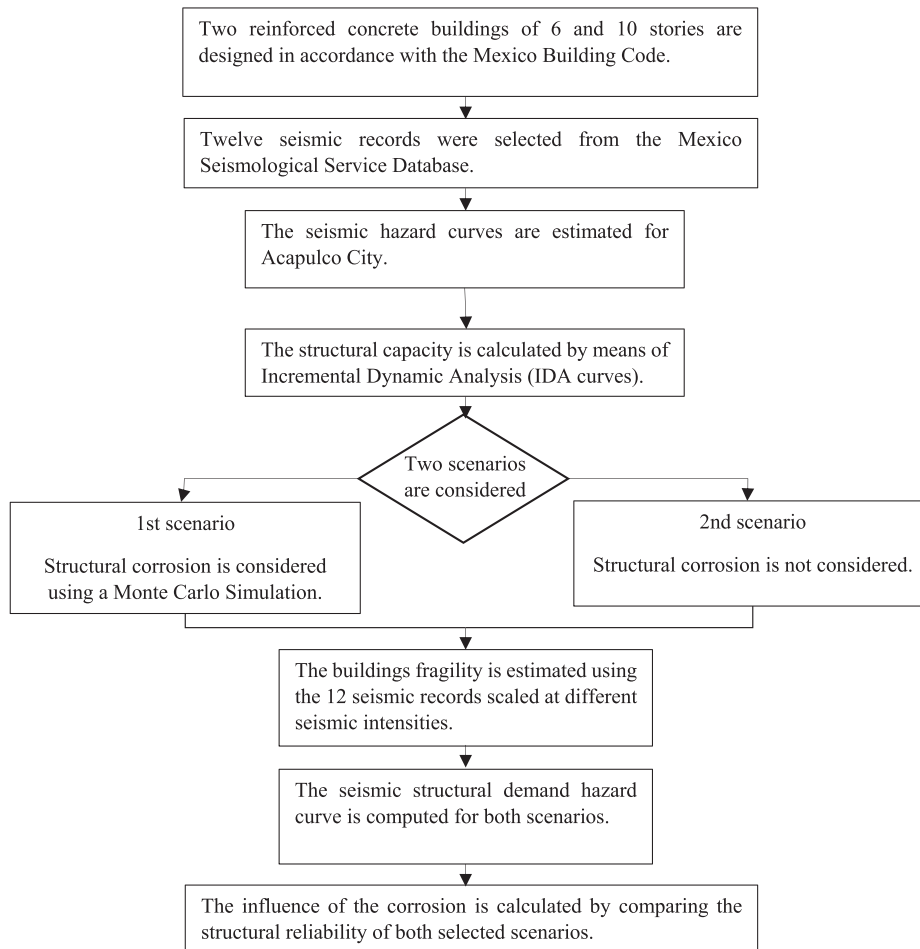


Fig. 2. Methodology Flowchart.

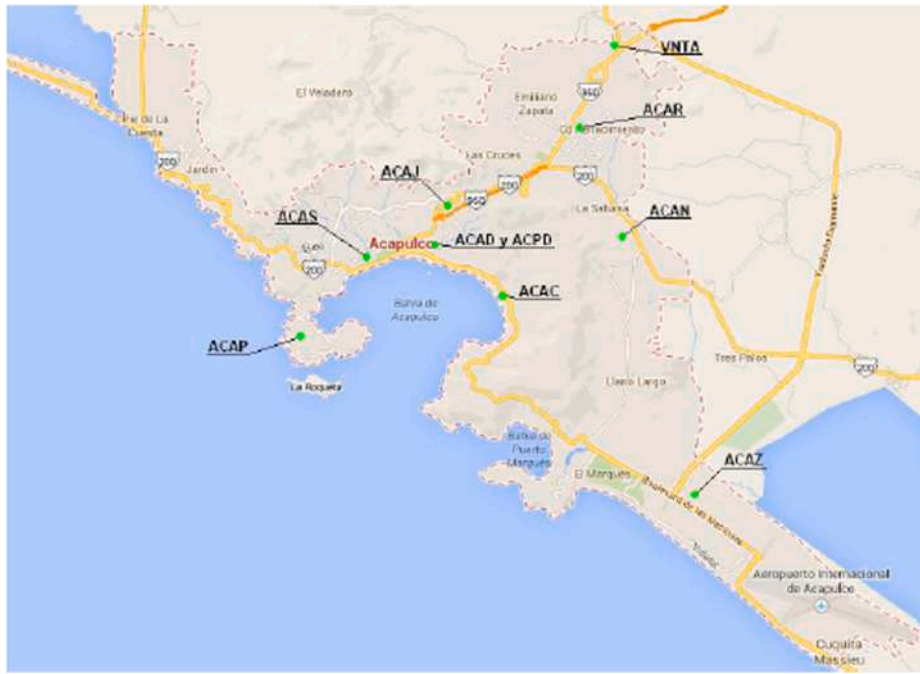


Fig. 3. Distribution of the seismic stations in Acapulco, Guerrero.

$$A(t) = \begin{cases} nD_0^2 \frac{\pi}{4} & \text{for } t \leq T_i \\ n[D(t)]^2 \frac{\pi}{4} & \text{for } T_i < t < T_i + D_0/C_{corr}i_{corr} \\ 0 & \text{for } t \geq T_i + D_0/C_{corr}i_{corr} \end{cases} \quad (4)$$

where n is the number of reinforcing steel bars; D_0 is the initial diameter of steel reinforcement; t is the elapsed time in years; C_{corr} is the rate of corrosion; i_{corr} is the corrosion density; and $D(t)$ is the reinforcement diameter at the end of t years, which can be represented by Eq. (5):

$$D(t) = D_0 - C_{corr}i_{corr}(t - T_i) \quad (5)$$

In this research a constant corrosion rate of 0.023 was adopted from Thoft-Christensen [29] which was identified from field data on existing concrete member of buildings in deicing salts, and the corrosion density is considered uniformly distributed for a medium deterioration level as shown in Table 1.

3. Methodology

The flowchart of Fig. 2 describes the methodology considered in the present study.

4. Structural reliability

The seismic structural demand hazard curve is expressed in terms of the maximum inter-story drifts (MID). The mean annual rate of exceeding a specific value of mid is estimated using the following expression [33,34]:

$$\nu(mid) = \int \left| \frac{d\nu(S_a)}{d(S_a)} \right| P(MID > mid|S_a) d(S_a) \quad (6)$$

where $\nu(mid)$ is the seismic demand hazard curve, which represents the average number of times per year that mid is exceeded; mid is the certain value of the maximum story drift; MID is the structural demand, represented by the maximum story drift; S_a is the pseudo-acceleration associated with the fundamental period of vibration of the building; $P(MID > mid|S_a)$ is the fragility curve, which is the conditional

Table 2
Seismic ground motion records.

Record	Name	Date	M	Coordinates of the epicentre (Lat, Long)
S1	ACAC9509.141 N00E	1995/09/14	6.4	16.31, 98.88
S2	ACAC9509.141 N90E	1995/09/14	6.4	16.31, 98.88
S3	ACAD1112.111 N00E	2011/12/11	6.5	17.84, 99.98
S4	ACAD1112.111 N90E	2011/12/11	6.5	17.84, 99.98
S5	ACAD9509.141 N00E	1995/09/14	6.4	16.31, 98.88
S6	ACAD9509.141 N90E	1995/09/14	6.4	16.31, 98.88
S7	ACAD9701.111 N00E	1997/01/11	6.9	17.91, 103.0
S8	ACAD9701.111 N90E	1997/01/11	6.9	17.91, 103.0
S9	ACAD9906.151 N00E	1999/06/15	6.4	18.18, 97.51
S10	ACAD9906.151 N90E	1999/06/15	6.4	18.18, 97.51
S11	ACAD9909.301 N00E	1999/09/30	7.5	15.95, 97.03
S12	ACAD9909.301 N90E	1999/09/30	7.5	15.95, 97.03

probability that MID exceeds the value of mid , given an intensity S_a ; and $\nu(S_a)$ is the seismic hazard curve of the site of interest, which represents the average number of times per year that a seismic ground motion occurs with an intensity equal to or greater than S_a .

4.1. Mean annual rate of structural failure

The structural reliability of the buildings is evaluated using the mean annual rate of structural failure (ν_f). It is given by [35,36]:

$$\nu_f = \int \left| \frac{d\nu_{MID}(mid)}{d(mid)} \right| P(C \leq mid) d(mid) \quad (7)$$

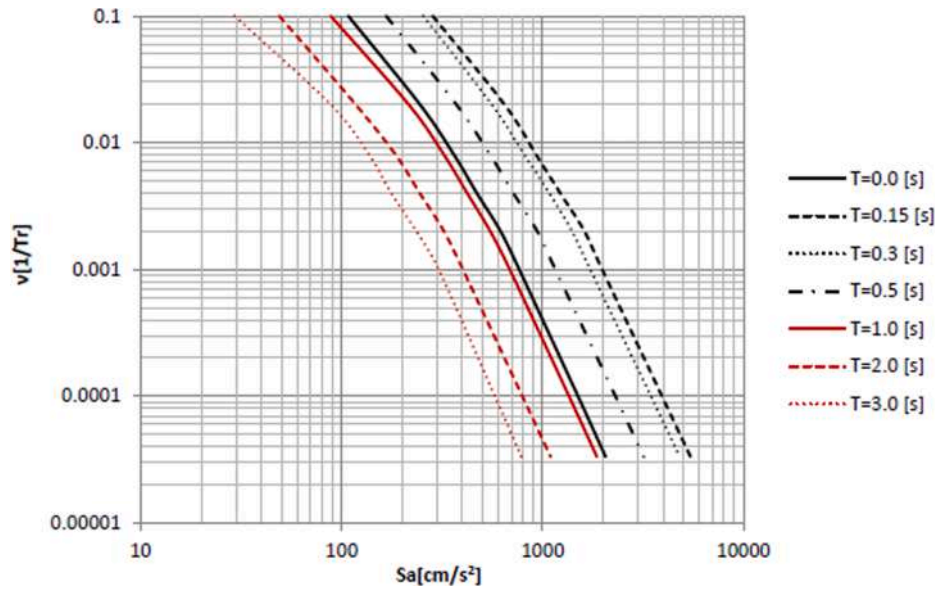


Fig. 4. Seismic hazard curves corresponding to COYC station.

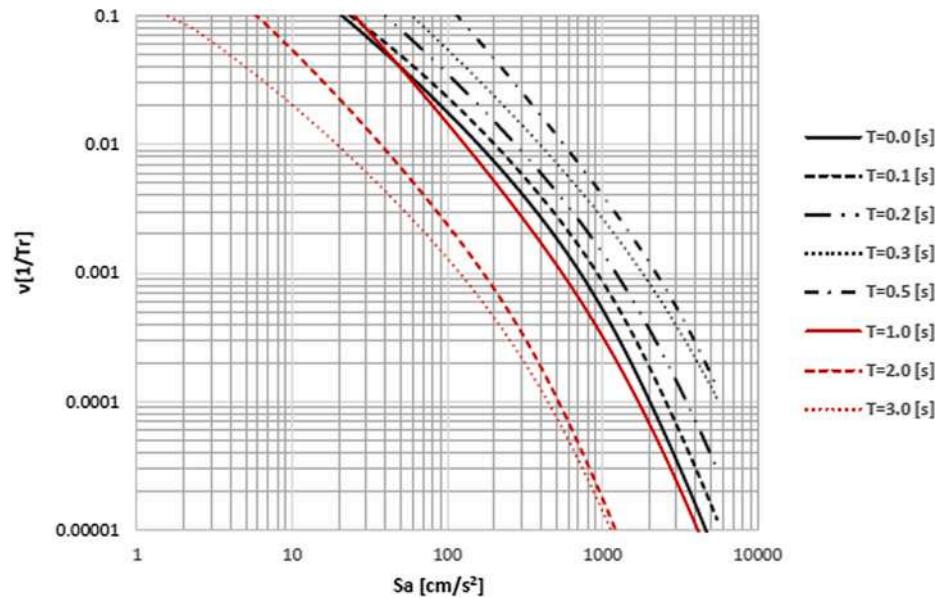


Fig. 5. Seismic hazard curves corresponding to ACAC and ACAD stations.

where ν_f is the mean annual rate of structural failure, which is the average number of times per year that the demand mid exceeds the capacity C ; and $P(C \leq mid)$ is the probability that the structural capacity C (close to collapse limit-state) be smaller than or equal to mid .

5. Earthquake ground motion records

The buildings are evaluated through incremental dynamic analysis (IDA) [37] with seismic ground motions near the coasts of Acapulco, Guerrero. The analyses were conducted using seismic records from two seismic stations: ACAC and ACAD, which are located in the area of soft soil on the coasts of Acapulco (see Fig. 3).

Table 2 shows the information of the selected earthquake ground motions recorded in the coast of Acapulco, Guerrero, for the seismic analyses of the RC buildings.

6. Seismic hazard study of Acapulco, Guerrero

From the seismic hazard curves included in the CFE Earthquake Design Manual of México, the curves for Acapulco, Guerrero were obtained through the formulation proposed by Esteva [33]. This formulation establishes that from the known seismic hazard curves of a particular site it is possible to determine the hazard curves for another place as long as there are seismic records obtained simultaneously at both sites. This is possible through the statistical parameters of the spectral ratios between both sites using the following expression:

$$\nu_Y(y) = \int_0^\infty \nu_X \frac{y}{z} f_z(z) dz = E_z \left(\nu_X \left(\frac{y}{z} \right) \right) \tag{8}$$

where $\nu_Y(y)$ is the mean annual rate of exceedance of a seismic intensity measure, for the recipient site; $\nu_X(y/z)$ is the mean annual rate of exceedance of a seismic intensity measure for the reference site, divided by the variable Z ; Z is the acceleration response spectral ratio (y/x), it refers

Table 3
Geometric characteristics of the building models.

Model	Number of spans in X direction	Number of spans in Y direction	story height
6 stories, M6	4 @ 8 m.	4 @ 8 m.	4 m.
10 stories, M10	4 @ 8 m.	4 @ 8 m.	4 m.

Table 4
Project data.

Seismic behaviour factor	Q = 2
Intended use of the building	Hotel
Concrete	Class 1: $f_c = 250 \text{ kg/cm}^2$
Reinforcing steel	$F_y = 4200 \text{ kg/cm}^2$
Serviciability peak inter-story drift	0.002
Collapse peak inter-story drift	0.015

to the ratio between the response spectra corresponding to the recipient and the reference sites; $f_Z(Z)$ is the pdf of Z.

Fig. 4 shows the seismic hazard curves corresponding to the COYC station (CFE Earthquake Design Manual) and in Fig. 5 the seismic hazard curves calculated period by period, belonging to the ACAC and ACAD stations.

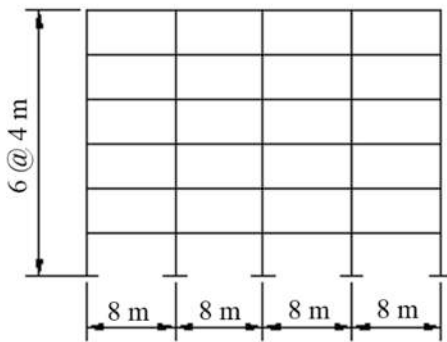


Fig. 6. Elevation and floor plan: six-story building.

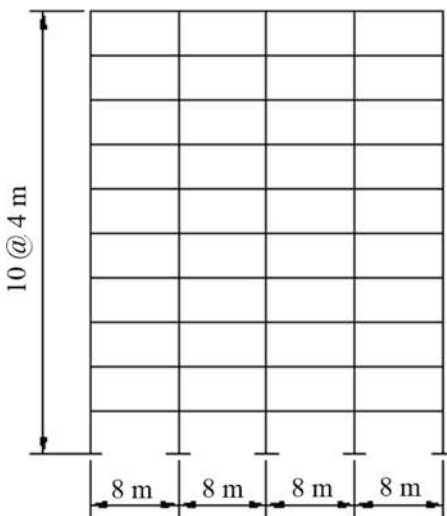


Fig. 7. Elevation and floor plan: ten-story building.

7. Structural models

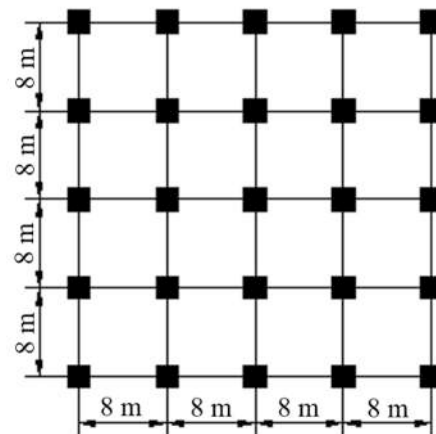
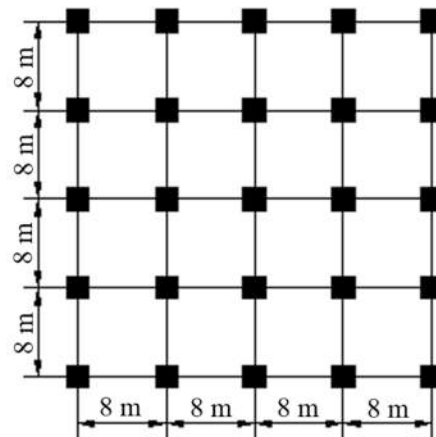
Two regular buildings are analyzed keeping the same layout configuration but varying the number of floors (six and ten stories), built with reinforced concrete with four eight-meter spans in both directions and with a height of four meters, located very close to the coastline in Acapulco, Guerrero, Mexico. The design was made under the criteria of the CFE Earthquake Design Manual of México.

Tables 3 and 4 show the geometric characteristics of the studied models and the project data used for design; Figs. 6 and 7 show the floor layout and building heights.

Figs. 8 and 9 illustrate the beams and columns sections of the six-story and ten-story buildings.

8. Results and discussion

In order to study the influence of the variation of the corrosion level for different cover depths, the structural reliability of the buildings over its useful lifetime was estimated for two covers depths, 5 cm cover main bar to the bottom, top and side, and 7 cm respectively. The corrosion initiation time (T_i) from Eq. (3) is used for this purpose. In order to evaluate each cover, ten simulations were performed through the Montecarlo technique, different results were obtained varying the parameters of Table 1. In the present study it was decided to make a total of



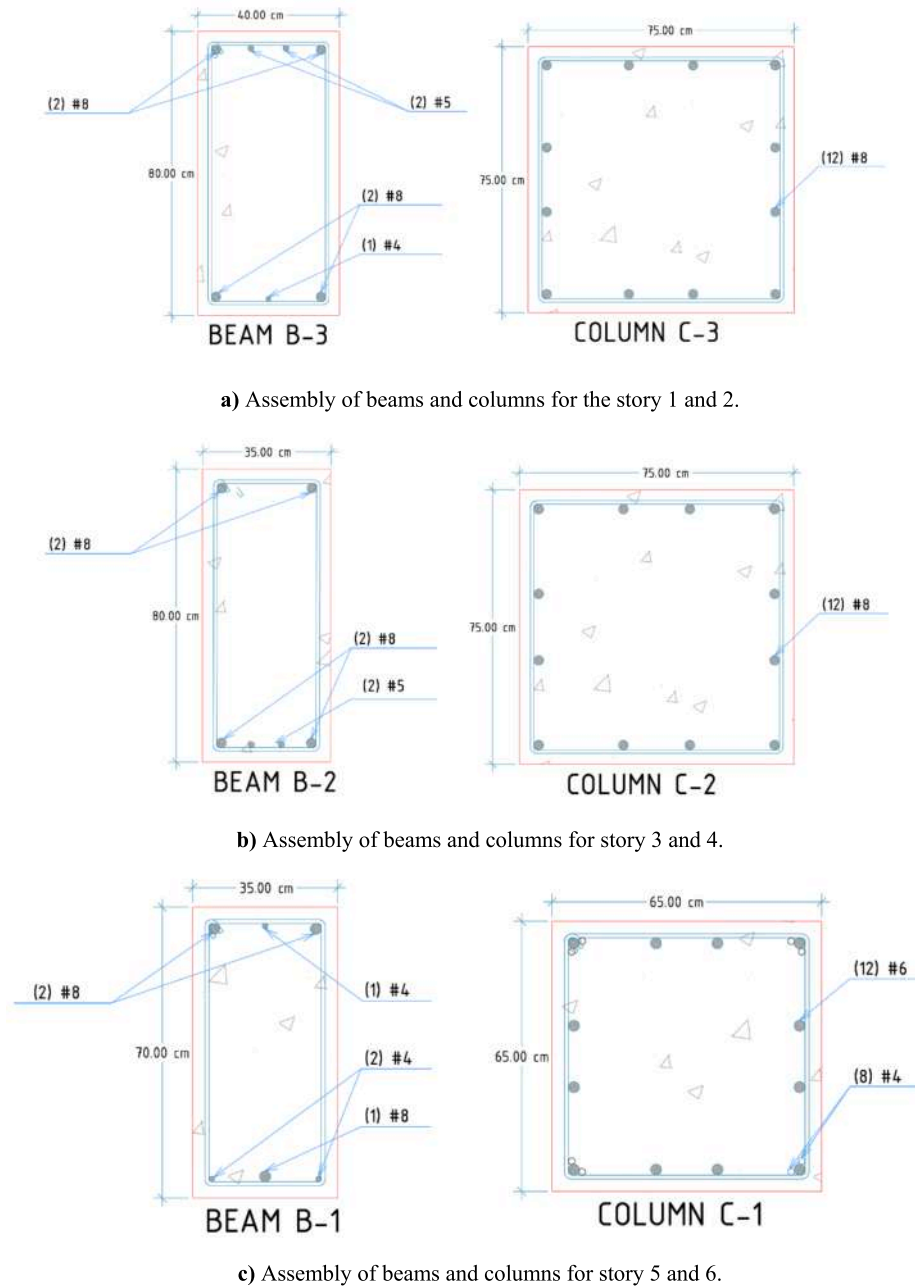


Fig. 8. Assembly of beams and columns for the M6 model.

10 simulations for each of the covers of 5 cm and 7 cm. The results are presented for each of the simulations in Fig. 10. It is shown a comparison between the corrosion initiation time for each of the covers, it can be seen that the corrosion initiation time is higher for the 7 cm cover.

8.1. Loss of cross sectional area

Table 5 illustrates the cross sectional area of the steel bars for models M6 before and after the corrosion initiates. As mentioned in previous chapters, the area loss is estimated using Eq. (4). In Table 5 the average reduction of the reinforced steel bars of the ten simulations for each section analyzed is shown in terms of area (cm²) and for the M6 model. Notice that for both models, it is considered that only the steel bars of the exterior frames are affected by corrosion. It can be seen that the cross sectional areas corresponding to the corrosion level of 1 year did not decrease considerably; such reduction was similar (around 2%) for all

sections. It is observed that for the corrosion level of 30 years after corrosion initiates, a considerable decrease of the cross sectional area has occurred, equivalent to approximately 70% for every section. Similar results were obtained for the M10 model but they were omitted for the sake of brevity.

8.2. Incremental dynamic analysis

The incremental dynamic analysis for different intensity levels was performed by a nonlinear step by step dynamic analysis using the RUAMOKO3D software [38]. The previously selected seismic records were scaled at different spectral acceleration values ranging from 0.1 to 1.2 g. As a result of this analyses the maximum inter-story drift for each structure and intensity level is obtained. In Fig. 11, the results of incremental dynamic analysis for the M6 model with 5 cm cover and ten years after its construction are compared. In addition, the results for the

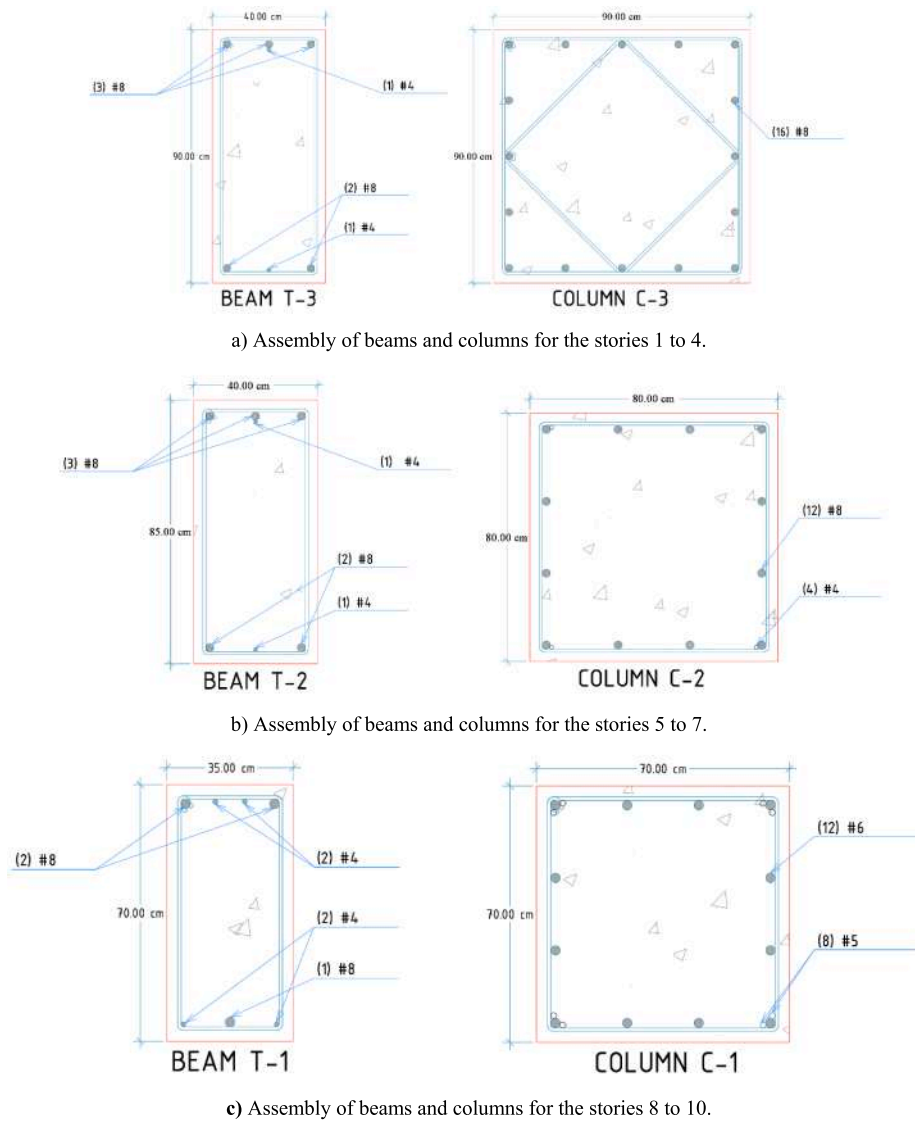


Fig. 9. Assembly of beams and columns for the M10 model.

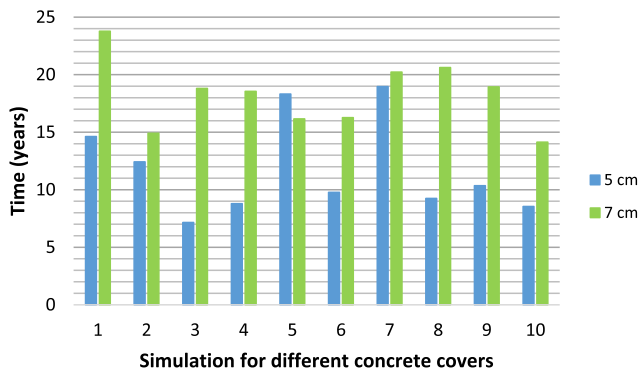


Fig. 10. Corrosion initiation time for different concrete covers.

same model but without the consideration of the corrosion effect are illustrated. It can be seen that the *MID* tend to increase as the level of intensity of the earthquake ground motion increases. It is important to mention that after ten years of corrosion the *MID* values are very similar, an increment about 3% is observed. Moreover, as it will be observed below if the time elapsed is greater than, for example, 30 years the

Table 5

Cross sectional area loss considering each section analyzed of the M6 model.

Section		Initial	T ₁ + 1 years	10 years	20 years	30 years
T40X80	as_ext ^{sup}	14.10	13.92	10.02	6.02	3.18
	as_loext ^{inf}	11.40	11.26	8.26	5.16	2.92
	as_cen ^{sup}	11.40	11.26	8.26	5.16	2.92
	as_cen ^{inf}	11.40	11.26	8.26	5.16	2.92
T35X80	as_ext ^{sup}	10.13	9.98	7.30	5.86	4.38
	as_ext ^{inf}	11.40	11.21	7.91	6.20	4.51
	as_cen ^{sup}	14.10	13.84	9.57	7.36	5.20
	as_cen ^{inf}	14.10	13.84	9.57	7.36	5.20
T35X70	as_ext ^{sup}	11.40	11.26	8.26	5.16	2.92
	as_ext ^{inf}	9.03	8.90	6.23	3.55	1.73
	as_cen ^{sup}	7.60	7.49	5.15	2.89	1.49
	as_cen ^{inf}	7.60	7.49	5.15	2.89	1.49
C75X75	as_col	60.80	60.15	45.52	29.69	17.35
C75X75	as_col	60.80	60.15	45.52	29.69	17.35
C65X65	as_col	44.34	43.62	28.43	13.94	5.23

difference can increase up to 12%.

The median values of the maximum inter-story drifts computed for the M6 model after twenty years of the corrosion initiation time are

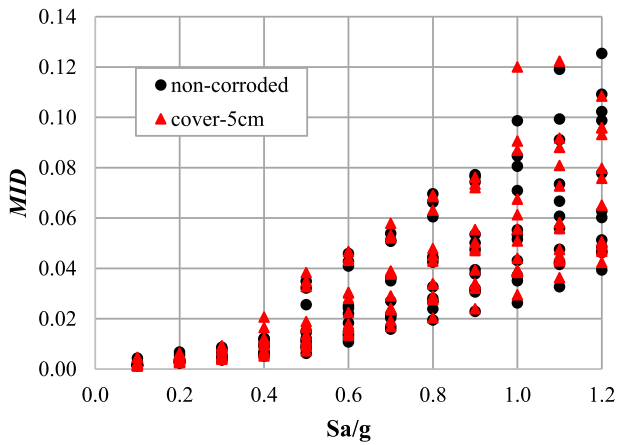


Fig. 11. IDA for the M6 model after ten years of corrosion.

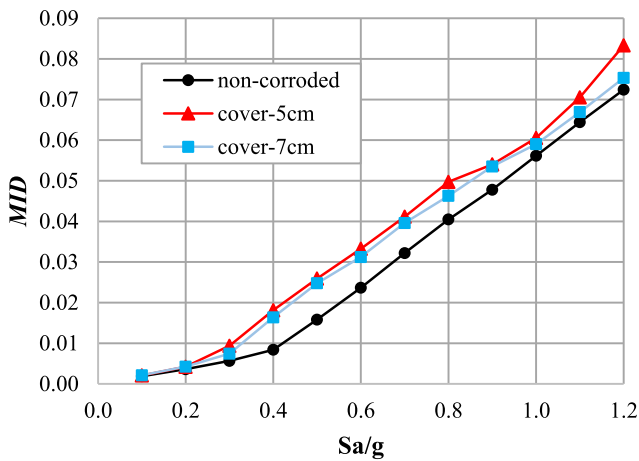


Fig. 12. Median values of the maximum inter-story drift for the M6 model after twenty years of corrosion.

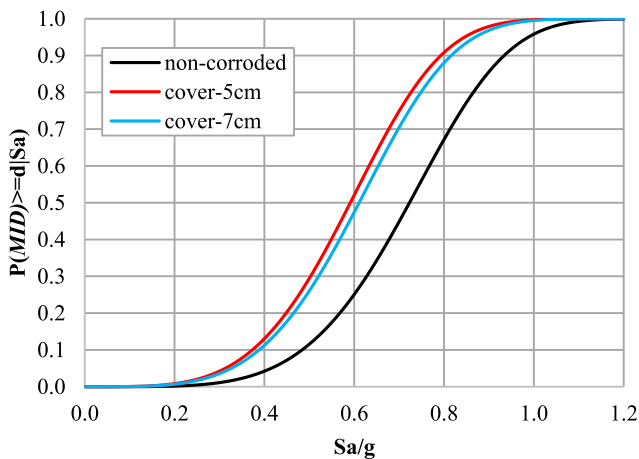


Fig. 13. Fragility curves for the M6 model after thirty years of corrosion.

shown in Fig. 12. The two different covers analyzed are considered. It can be seen that after this time elapsed the difference between the non-corroded and the 5 cm cover are high; for example, for a value of $Sa/g = 0.6$ a 29% difference is observed. It is also observed that the difference between the two covers considered is small for values of intensity measures smaller than 1 g, but the difference tends to increase for higher levels of intensity.

Table 6

Probability of exceeding the collapse prevention limit state (intensity level of 0.6 g).

Time	Cover	Sa/g	$P(D \geq d Sa/g)$
(10 years)	5 cm	0.6	32.2%
	7 cm		29%
	Non-corroded		25.09%
(20 years)	5 cm	0.6	42.5%
	7 cm		39.4%
	Non-corroded		25.09%
(30 years)	5 cm	0.6	52.1%
	7 cm		47.4%
	Non-corroded		25.09%

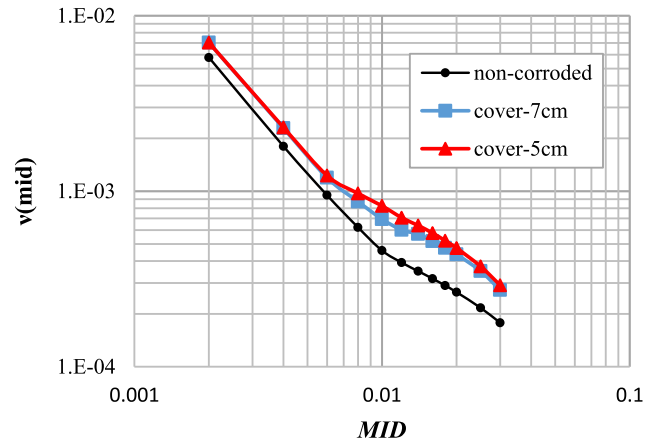


Fig. 14. Maximum inter-story drift demand hazard curve for the 6-story building after 30 years of construction.

8.3. Fragility curves

Fragility curves were developed at the damage control and the collapse prevention limit states for the two models after 10, 20 and 30 years. In addition to compare the fragility curves themselves the different covers are considered. Fig. 13 shows the comparison between fragility curves for a peak inter-story drift of 0.03 (collapse prevention) of the 6-story building with a 5 cm and 7 cm cover after 30 years of its construction. The black curve represents the building without corrosion, while the blue and red curves represents the building affected by corrosion. It can be observed that the conditional probability of exceedance is higher as the intensity level increases. For example, Fig. 13 shows that for the intensity of 0.6 g, the 7 cm curve has a probability of exceedance of 47%, while for the non-corroded curve the probability is only 24%. This means that the building after 30 years of construction has nearly twice as likely to exceed a drift of 0.03 compared to a non-corroded building.

The summary of the fragility analysis can be seen in Table 6, it is only shown the M6 model for a $Sa/g = 0.6$ for the sake of brevity. From the results of the fragility analysis, it is noticed that the system experiences a significant increase in the structural fragility over time. For example, the probability of exceeding the collapse limit state increases from 32% to 52% (from 10 years to 30 years) for a 5 cm cover at an intensity level of 0.6 g. It is important to say that the increase in the seismic fragility with age is also present in the damage control limit state.

8.4. Seismic demand hazard curves

The seismic demand hazard curves represent the mean annual rate of exceeding the maximum inter-story drift. These curves were obtained by numerical integration of Eq. (6). Fig. 14 shows the demand hazard

Table 7
Mean annual rate of exceeding the two limit states considered for the M6 model.

		Cover	Mean $\nu(mid)$	T_r (years)
Damage control 0.01	10 years	Non-corroded	0.00046	2179
		5 cm	0.00051	1959
		7 cm	0.00055	1824
	20 years	Non-corroded	0.00046	2179
		5 cm	0.00061	1639
		7 cm	0.00062	1622
	30 years	Non-corroded	0.00046	2179
		5 cm	0.00072	1383
		7 cm	0.00088	1141
Collapsed prevention 0.03	10 years	Non-corroded	0.00018	5622
		5 cm	0.00020	5085
		7 cm	0.00021	4780
	20 years	Non-corroded	0.00046	5622
		5 cm	0.00024	4132
		7 cm	0.00026	3847
	30 years	Non-corroded	0.00046	5622
		5 cm	0.00029	3499
		7 cm	0.00031	3267

Table 8
Mean annual rate of exceeding the two limit states considered for the M10 model.

		Cover	Mean $\nu(mid)$	T_r (years)
Damage control 0.01	10 years	Non-corroded	0.000989	1011
		5 cm	0.001079	927
		7 cm	0.001147	872
	20 years	Non-corroded	0.000989	1011
		5 cm	0.001505	665
		7 cm	0.001574	635
	30 years	Non-corroded	0.000989	1011
		5 cm	0.001789	559
		7 cm	0.001780	562
Collapsed prevention 0.03	10 years	Non-corroded	0.000130	7683
		5 cm	0.000132	7569
		7 cm	0.000131	7610
	20 years	Non-corroded	0.000130	7683
		5 cm	0.000133	7508
		7 cm	0.000126	7922
	30 years	Non-corroded	0.000130	7683
		5 cm	0.000126	7917
		7 cm	0.000120	8324

curves for the M6 model after 30 years of construction for the two considered covers. The black curve represents the non-corroded building while the red and blue represent the 5 cm and 7 cm covers, respectively. From Fig. 14 it can be seen that for the non-corroded model the mean annual rate of exceeding the damage control limit state (0.01) is equal to 0.00046 corresponding to a recurrence interval of 2179 years ($T_R = 1/\nu$), while for the collapse prevention limit state $\nu(0.03) = 0.00018$ or a recurrence interval of 5555 years. When the comparison is for the same building but considering corrosion, the differences are up to 30% and 58% for the damage control and collapse prevention limit states, respectively. It is also observed that for small values of MID the differences are small; this is because the structure remains in the elastic range.

The differences increase as the MID increases. The summary of all the results of the average of the ten simulations of corrosion is shown in Tables 7 and 8. Notice from these tables that the conclusions made for the M6 model are similar to those of the M10 model.

9. Conclusions

The structural reliability was evaluated at the end of different time intervals considering the variation of the structural capacity and the structural demand due to the corrosion for two reinforced concrete buildings with 6 and 10 stories. The buildings are located in the City of Acapulco in Mexico and the drift demand hazard curves are evaluated using several earthquake ground motions. The effects of corrosion on reinforced concrete structures can be divided into four important points: the first one is when the penetration of chlorides occurs where the structure is not compromised; the second one when the concentration of chlorides in the surface of the reinforcing steel reaches a critical concentration which initiates its corrosion, at this point it is when the structure begins to deteriorate, during the third point the corrosion of the steel continues to evolve and the fourth point is when the cracking occurs in the section. It should be mentioned that the phenomenon of corrosion continues, therefore, reinforcing steel bars continues with degradation and this could become a problem for the structural capacity.

This study highlights the importance of taking into account the phenomenon of corrosion for reinforced concrete structures that are close to a marine environment, where this phenomenon is most frequently presented by the penetration of chlorides. The results show that the effect of corrosion significantly affects the seismic fragility and reliability of buildings; furthermore, the seismic demand hazard curves are significantly different up to 55% when a concrete cover of 5 cm is considered (which is a typical practice). The differences between each cover 5 cm and 7 cm are small for about 5% so it is recommended that the concrete cover should not exceed 5 cm. It is important to mention that this corrosion effect is currently neglected in building codes so this could lead to erroneous estimation of the structural capacity and reliability of buildings near salt environments.

CRedit authorship contribution statement

Juan Bojórquez: Conceptualization, Methodology, Software, Writing - original draft, Supervision, Writing - review & editing, Project administration, Funding acquisition. **Sandra Ponce:** Methodology, Software, Investigation, Formal analysis, Data curation. **Sonia E. Ruiz:** Resources, Conceptualization, Supervision. **Edén Bojórquez:** Conceptualization, Writing - original draft, Supervision, Validation, Project administration, Writing - review & editing. **Alfredo Reyes-Salazar:** Validation, Visualization, Supervision. **Manuel Barraza:** Writing - review & editing, Formal analysis. **Robespierre Chávez:** Software, Investigation. **Federico Valenzuela:** Methodology, Visualization. **Herian Leyva:** Software, Writing - review & editing. **Victor Baca:** Formal analysis, Data curation.

Declaration of Competing Interest

The authors declare that they have no known competing financial interests or personal relationships that could have appeared to influence the work reported in this paper.

Acknowledgements

The support given by Consejo Nacional de Ciencia y Tecnología (CONACYT) to the first author under Grant CB-2016-287103 is appreciated. This research had the support of Universidad Autónoma de Sinaloa under grant PROFAPI and Universidad Nacional Autónoma de México under Project DGAPA-PAPIIT-IN100320.

References

- [1] Aguirre AM, Mejía de Gutiérrez R. Durabilidad del hormigón armado expuesto a condiciones agresivas. *Materiales de Construcción* 2013;7–38.
- [2] Tolentino D, Carrillo CA. Evaluation of structural reliability for reinforced concrete buildings considering the effect of corrosion. *KSCE J Civ Eng* 2017;22:1–10.
- [3] Del Valle A, Pérez T, Martínez M. El fenómeno de la corrosión en estructuras de concreto reforzado. Sanfandila, Querétaro: Secretaría de Comunicaciones y Transporte, Instituto Mexicano del Transporte; 2001.
- [4] Thoft-Christensen P. Deterioration of concrete structures. In: *Fist international conference on bridge maintenance, safety and management, IABMAS 2002*, Barcelona, Spain; p. 1501–8.
- [5] Di Lorenzo G, Rizzo F, Formisano A, Landolfo R, Guastaferrò A. Corrosion wastage models for steel structures: literature review and a new interpretative formulation for wrought iron alloys. *Key Eng Mater* 2019;813:209–14. <https://doi.org/10.4028/www.scientific.net/KEM.813.209>.
- [6] Bossio A, Lignola GP, Protà A. An overview of assessment and retrofit of corroded reinforced concrete structures. *Procedia Struct Integrity* 2018;11:394–401. <https://doi.org/10.1016/j.prostr.2018.11.051>.
- [7] Rizzo F, Di Lorenzo G, Formisano A, Landolfo R. Time-dependent corrosion wastage model for wrought iron structures. *J Mater Civ Eng* 2019;31(8):04019165. [https://doi.org/10.1061/\(ASCE\)MT.1943-5533.0002710](https://doi.org/10.1061/(ASCE)MT.1943-5533.0002710).
- [8] Khampanit A, Leelataviwat S, Kochanin J, Warnitchai P. Energy-based seismic strengthening design of non-ductile reinforced concrete frames using buckling-restrained braces. *Eng Struct* 2014;81:110–22. <https://doi.org/10.1016/j.engstruct.2014.09.033>.
- [9] Formisano A, De Matteis G, Panico S, Calderoni B, Mazzolani FM. Full-scale test on existing RC frame reinforced with slender shear steel plates. In: *Proc. of the 5th international conference on behavior of Steel Structures in Seismic Areas (STESSA)*, Yokohama, Japan; 2006. p. 827–834.
- [10] Formisano A, Mazzolani FM, De Matteis G. Numerical analysis of slender steel shear panels for assessing design formulas. *Int J Struct Stab Dyn* 2017;7(2):273–94. <https://doi.org/10.1142/S0219455407002289>.
- [11] Jarrahi H, Asadi A, Khatibinia M, Etedali S. Optimal design of rotational friction dampers for improving seismic performance of inelastic structures. *J Build Eng* 2020;27:100960. <https://doi.org/10.1016/j.jobe.2019.100960>.
- [12] Andrade AC. Cover cracking as a function of bar corrosion: Part I-Experimental test. *Mater Struct* 1993;453–64.
- [13] Liu Y, Weyers RE. Modeling the Time-to-Corrosion cracking in chloride contaminated reinforced concrete structures. *ACI Mater J* 95-M65; 1998.
- [14] Castañeda H, Castro P, González C, Genescá J. Modelo de difusión de cloruros en las estructuras de hormigón armado expuestas en la Península de Yucatán (México). *Revista de Metalurgia* 1997;387–92.
- [15] Firouzi A, Taki A, Mohammadzadeh S. Time-dependent reliability analysis of RC beams shear and flexural strengthened with CFRP subjected to harsh environmental deteriorations. *Eng Struct* 2019;196. <https://doi.org/10.1016/j.engstruct.2019.109326>.
- [16] Shin K, Kim J, Lee K. Probability-based durability design software for concrete structures subjected to chloride exposed environments. *Comput. Concr.* 2011;8: 511–24.
- [17] Ryan P, O'Connor A. Probabilistic analysis of the time to chloride induced corrosion for different self-compacting concretes *Constr. Build. Mater.* 2013;47: 1106–16.
- [18] Nogueira C, Leonel E. Probabilistic models applied to safety assessment of reinforced concrete structures subjected to chloride ingress. *Eng. Fail. Anal.* 2013; 31:76–89.
- [19] Akiyama M, Frangopol DM, Matsuzaki H. Life-cycle reliability of RC bridges piers under seismic and airborne chloride hazard. *Earthquake Eng Struct Dyn* 2011;40: 1671–87.
- [20] Chen GM, Teng JG, Chen JF. Shear strength model for FRP-strengthened RC beams 596 with adverse FRP-steel interaction. *J Compos Constr* 2012;17:50–66.
- [21] De Domenico D, Pisano AA, Fuschì P. Limit analysis on FRP-strengthened RC 599 members. *Frattura ed Integrità Strutturale* 2014;8:209–21.
- [22] Abbasloo AA, Shayanfar MA, Pahlavan H, Barkhordari MA, Hamze-Ziabari SM. Prediction of shear strength of FRP-reinforced concrete members using a rule-based method. *Mag Concr Res* 2018:1–6.
- [23] Shang X, Zhang Y, Qu N, Tang X. Electrochemical analysis of passivation film formation on steel rebar in concrete. *Int J Electrochem Sci* 2016;11:5870–6. <https://doi.org/10.20964/2016.07.44>.
- [24] Ouzaa K, Oucif C. Numerical model for prediction of corrosion of steel reinforcements in reinforced concrete structures. *Undergr Space* 2018;4. <https://doi.org/10.1016/j.undsp.2018.06.002>.
- [25] Homan L, Ababneh A, Xi Y. The effect of moisture transport on chloride penetration in concrete. *Constr Build Mater* 2016;125:1189–95.
- [26] Zhu X, Zi G. A 2D mechano-chemical model for the simulation of reinforcement corrosion and concrete damage. *Constr Build Mater* 2017;137:330–44.
- [27] Ossorio A, Raydel L. Predicción de la vida útil de estructuras de hormigón armado mediante la utilización de un modelo de difusión de cloruro. *Revista Facultad de Ingeniería Universidad de Antioquia* 2014;161–72.
- [28] Thoft-Christensen P. What happens with reinforced concrete structures when the reinforcement corrodes. In: *Second international workshop on "Life-Cycle cost analysis and design of civil infrastructure systems*, Ube Yamaguchi, Japan; 2001. p. 35–46.
- [29] Thoft-Christensen P. Modelling of corrosion cracks. In: *IFIP TC7 conference*, Sophia Antipolis, France; 2003. p. 1501–8.
- [30] Li CQ, Mahmoodian M. Risk based service life prediction of underground cast iron pipes subjected to corrosion. *Reliab Eng Syst Saf* 2013;119:102–8.
- [31] Cook DC, Van Orden AC, Reyes J, Oh SJ, Balasubramanian R, Carpio JJ, et al. Atmospheric corrosion in marine environments along the Gulf of México. *Marine corrosion in tropical environments*. West Conshohocken: American Society for Testing and Materials; 2000.
- [32] Ni Choine M. Seismic reliability assessment of aging integral bridges. PhD thesis Trinity College Dublin; 2014.
- [33] Esteve L. Bases para la formulación de decisiones de diseño sísmico. *Facultad de Ingeniería, UNAM, México: Tesis de Doctorado*; 1968.
- [34] Cornell CA. Engineering seismic hazard analysis. *Bull Seismol Soc Am* 1968;58: 1583–606.
- [35] Cornell CA, Jalayer F, Hamburger RO, Foutch DA. The probabilistic basis for the 2000 SAC/FEMA steel moment frame guidelines. *J Struct Eng* 2002;128:526–33. [https://doi.org/10.1061/\(ASCE\)0733-9445\(2002\)128:4\(526\)](https://doi.org/10.1061/(ASCE)0733-9445(2002)128:4(526)).
- [36] Torres MA, Ruiz SE. Structural reliability evaluation considering capacity degradation over time. *Eng Struct* 2007;29:2183–92.
- [37] Vamvatsikos D, Cornell CA. Incremental dynamic analysis. *Earthquake Eng Struct Dyn* 2002;31:491–514. <https://doi.org/10.1002/eqe.141>.
- [38] Ruaumoko Carr AJ. Dynamic nonlinear analysis. Christchurch, New Zealand: Department of Civil Engineering, University of Canterbury; 2015.